Effects of High-frequency Microforging on the Laser Cladding Layer Prepared on the 304 Stainless Steel Substrate

Zhu Hongmei Yin Quan Peng Rushu

School of Mechanical Engineering, University of South China, Hengyang, Hunan 421001, *China*

Abstract The laser cladding layer on the 304 stainless steel surface is modified by a high-frequency microforging process. The microstructure and phase constitution of the laser cladding layer before and after the high-frequency microforging treatment are characterized by using optical microscopy and X-ray diffraction. The microhardness distribution and corrosion property of the counterparts are examined by Vickers microhardness tester and the electrochemical work station, respectively. The results show that laser cladding layer is of a broken dendritic microstructure and refined grain size after microforging, while there is no obvious change in the phase constitution. The microhardness of the microforged area is greatly enhanced with an affected depth of 0.65 mm. The average microhardness of the surface is improved by about 30% and the microhardness increment decreases gradually with the increasing distance from the top of the cladding layer. The corrosion resistance of the laser cladding layer is improved by nearly two folds after microforging.

Key words laser technique; laser cladding; high-frequency microforging; microstructure; microhardness; corrosion resistance

OCIS codes 140.3390; 350.3850; 160.3900

高频微锻造处理对304不锈钢表面激光熔覆层的影响

朱红梅 尹 泉* 彭如恕

南华大学机械工程学院, 湖南 衡阳 421001

摘要 对304不锈钢基材表面制备的激光熔覆层进行了高频微锻造处理。通过光学显微镜和X射线衍射仪分别研究了高频微锻造处理前后激光熔覆层的显微组织和相组成,利用显微维氏硬度计和电化学工作站分别对其进行了显微硬度测试和耐腐蚀性能测试。结果表明:经过高频微锻造处理后,激光熔覆层中的枝晶组织得到破碎,晶粒变细,但相组成无明显变化;微锻造作用区的显微硬度明显提高,影响深度为0.65 mm,表层硬度提高了约30%,高频微锻造处理对激光熔覆层的硬度影响程度随着距表层距离的增加而下降;激光熔覆层的耐腐蚀性能经微锻造处理后得到改善,为原始的2倍。

关键词 激光技术; 激光熔覆; 高频微锻造; 显微组织; 显微硬度; 电化学腐蚀

中图分类号 TG178 **文献标识码** A

doi: 10.3788/LOP52.121401

1 Introduction

Laser cladding technology is an important surface modification method to enhance the wear resistance, corrosion resistance and high-temperature oxidation resistance of materials, which has received much attentions in recent years[1-2]. However, defects such as pores and cracks occur readily in the laser cladding layer due to factors namely a non-equilibrium solidification process and the performance discrepancy between the coating and the substrate[3-4].

The high-frequency microforging technology is to input the metal materials with the vibrational energy by the punch of the ultrasonic generator. Consequently, the surface strength and mechanical properties of

收稿日期: 2015-02-28; **收到修改稿日期**: 2015-05-29; **网络出版日期**: 2015-11-26

基金项目: 国家自然科学基金(51201088)、湖南省自然科学基金(2015JJ3109)、南华大学青年英才支持计划(2014002)

作者简介: 朱红梅(1982—),女,博士,副教授,主要从事激光表面改性方面的研究。E-mail: meizihong999@126.com

*通信联系人。E-mail: yinquan_106@126.com

metal are improved due to the microstructural modification by the elasticoplastic deformation under the high-energy impact on the metal materials[5]. To date, ultrasonic impact treatment has been considered to be a controllable and convenient method to strengthen the welded joints of various materials[6]. It is demonstrated by Qiu that the residual stress of the laser prototyped 304 stainless steel coating on the Q235 substrate can be transformed from tensile stress into compressive stress after microforging by a strip cutting method[7]. In this paper, a iron-based laser cladding layer reinforced by Ti (C,N) particles is firstly prepared on the surface of 304 stainless steel. Then, a high-frequency microforging treatment is used to explore the effects on the microstructure and property of the laser cladding layer.

2 Experimental procedure

304 stainless steel is used as the base material with the size of 60 mm×40 mm×6 mm. Before the laser cladding, the substrate is firstly ground by the sandpaper to remove the oxide layer on the surface, then washed by absolute alcohol, and finally sandblasted by silica sand with the size of 60~80 mesh.

The laser cladding powder is a mixture of the dominant 304 stainless steel powder together with a 10% mixed powder (mass fraction) by the ilmenite (Fe-70%Ti) and pure graphite (99.9%) in a molar ratio of 1∶1. The aforementioned laser cladding powder is uniformly mixed by a ball mill for 10 min with an average size of 200 mesh. Then, the mixed powder is pre-coated on the substrate with a thickness of 1 mm by the organic adhesive.

A 5 kW TJ-T5000 CO_2 laser is used for the laser cladding process, and the parameter is as follows: the powder of 2.2 kW, scanning speed of 6 mm/s, the light spot diameter of 3 mm, overlap rate of 33%. Pure nitrogen gas is blown for both the lateral protection and the reaction gas with the flow rate of 10 L/min. A ZJ-II type ultrasonic impact machine is used for the microforging treatment with a frequency of 20 kHz. To study the effects of high-frequency microforging on the microstructure and properties of the laser cladding specimen, a GX-51F optical microscope (OM) and XD-6 X-ray diffraction (XRD) are used for the microstructure observation and phase analysis. The microhardness is measured by a HXD-1000B Vickers microhardness tester with a load weight of 200 g and a load time of 15 s. The corrosion property is tested by a CS300 electrochemical workstation and a 3.5% NaCl solution is adopted as the corrosion environment.

3 Results and discussion

Figure 1 compares the optical microscope microstructure of specimens before and after microforging. In appearance, the laser cladding layer on the 304 stainless steel becomes much brighter and smoother after a high-frequency microforging treatment. Without apparent defects such as pores and cracks, both the specimens are composed of three zones with distinct morphologies, namely cladding layer, transition region and substrate. The cladding layers maintain a good metallurgical combination with the substrate. It is noted that the dendritic crystal along the direction of heat flow in the cladding layer has been broken and refined after microforging.

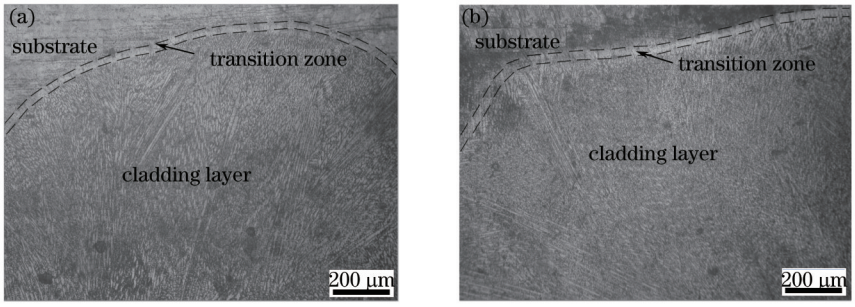

Fig.1 Optical microscope microstructure of specimens before and after microforging. (a) Before microforging; (b) after microforging

Figure2 shows the XRD patterns of the laser cladded specimens before and after microforging. It is obvious that there is no change in the phase constitution after a high-frequency microforging treatment. Both the cladding layers consist of phases Fe-Cr-Ni, γ-Fe, α-Fe, Ti($C_{0.3}N_{0.7}$) and Fe-N. Table 1 lists the corresponding full width at half maximum (FWHM) of the main XRD peaks for specimens before and after microforging. Apparently, the FWHM is enhanced for each diffraction peak after microforging. Additionally, the peaks have been widen and moved slightly to the direction of high diffraction angle for the microforged specimen. This is due to the grain refinement and lattice distortion, which suggests that a severe plastic deformation and microscopic compressive stress is presented in the cladding layer after microforging[8].

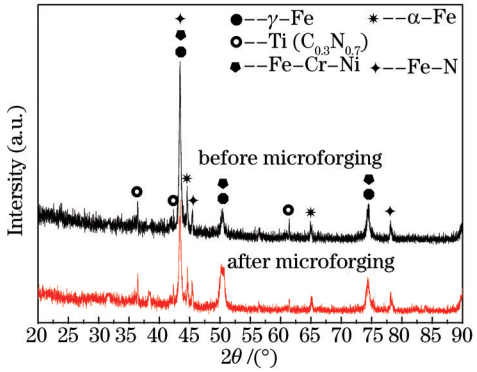

Fig.2 XRD patterns of specimens before and after microforging.

Table 1 FWHM of the main X-ray diffraction peaks for specimens before and after microforging

	Before microforging				After microforging			
2θ /(°)	36.286	43.420	50.420	74.341	36.461	43.490	50.730	74.432
Peak value/counts	60	820	120	138	149	509	194	140
FWHM	0.046	0.286	0.300	0.292	0.104	0.313	0.897	0.559

Figure 3 shows the microhardness variation with the depth from the surface of specimens. As clearly been seen, the microhardness of the as-received laser cladding layer is around 450 HV with the depth of 900 μm and then decreases gradually in the transition zone until 250 HV in the substrate before microforging. In contrast, the peak hardness of the cladding layer for the microforged specimen is 610 HV and the average surface microhardness is enhanced by about 30% after microforging. Unlike the plateau distribution in the cladding layer for the as-received laser cladded specimen, the microhardness is reduced successively with the depth from the surface of the microforged specimen. The reason for such a microhardness variation is due to the fact that the amount of plastic deformation decreases correspondingly with the increasing depth from the surface of the microforged specimen. The increase in the dislocation density and grain refinement are responsible for the increased microhardness of the cladding layer in the microforged specimen[6,9].

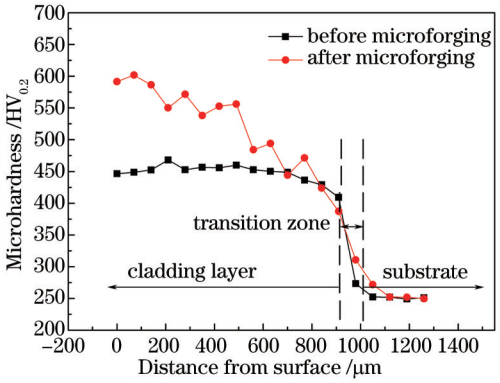

Fig.3 Comparison of the microhardness distribution of the laser cladded specimens before and after microforging

Figure 4 shows the potentiodynamic polarization curves of specimens before and after microforging

and the test results including corrosion potential (E_{corr}), corrosion current density (I_{corr}) and corrosion rate determined through the polarization curves are summarized in Table 2. Apparently, the corrosion potential is increased by 0.04123 V, the corrosion current density is decreased by 1.1413×10^{-7} A/cm^2 and the corrosion rate is lowered by 49.9% after microforging. According to Faraday′s law and graphical analysis of polarization curves, higher corrosion potential is equivalent to higher corrosion resistance and lower corrosion current density means lower corrosion rate[6]. Therefore, the corrosion resistance of the laser cladding layer is improved by a high-frequency microforging treatment.

In a 3.5%NaCl solution, there are the main following chemical reactions for specimens: $Fe\rightarrow Fe^{2+}+2e^-$ (anodic reaction), $2H_2O+2e^-\rightarrow H_2+OH^-$ (cathodic reaction), $Fe^{2+}+2OH^-\rightarrow Fe(OH)_2\downarrow$, $4Fe(OH)_2+2H_2O+O_2\rightarrow 4Fe(OH)_3\downarrow$. The generated passivation film of $Fe(OH)_2$ and $Fe(OH)_3$ is easily destroyed by the anion such as Cl^-. It is well known that there is internal stress induced by the growth of such oxide film and a tensile stress is produced for iron oxide film[10]. The tensile stress increases with the increasing volume of the oxide film until its rupture, and thus the corrosion rate is accelerated accordingly. However, a compressive stress can be produced on the material surface by a high-frequency microforging treatment[5-6]. It is therefore that the passivation film can not be easily damaged due to the increased lateral compressive stress, and thus the corrosion resistance of specimen is improved. In addition, the grain refinement is also the factor for the improvement in the corrosion resistant of specimen after microforging[11].

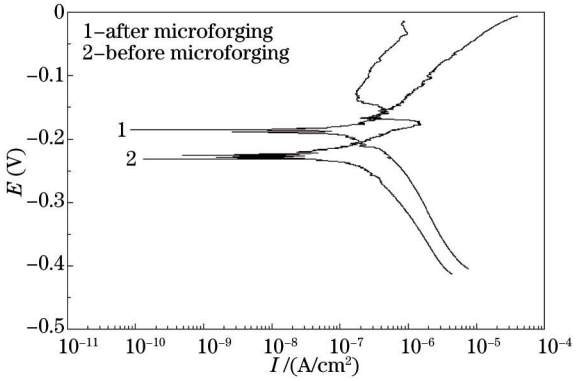

Fig.4 Potentiodynamic polarization curves tested in 3.5% NaCl solution at room temperature for specimens before and after microforging

Table 2 Electrochemical corrosion test results of specimens before and after microforging

Sample	E_{corr} /V	I_{corr} /(A/cm^2)	Corrosion rate /(mm/year)
Before microforging	−0.22618	2.3428×10^{-7}	2.7205×10^{-3}
After microforging	−0.18495	1.2015×10^{-7}	1.3626×10^{-3}

4 Conclusions

1) A deformation strengthening effect and grain refinement of the laser cladding layer is produced by a high-frequency microforging treatment. The microhardness of the microforged area is greatly enhanced with an affected depth of 0.65 mm. The microhardness increment decreases gradually with the increasing distance from the top of the cladding layer and the average microhardness of the surface is improved by about 30%.

2) The corrosion resistance of the laser cladding layer is improved by nearly two folds after microforging. The corrosion potential is increased by 0.04123 V and the corrosion current density is decreased by 1.1413×10^{-7} A/cm^2, which is due to the induced compressive stress and grain refinement by microforging.

References

1 Steffen N, Lutz M B, Jörg S. Coatings by laser cladding[J]. Comprehensive Hard Materials, 2014, 1: 507-525.

2 Wang Yanfang, Xiao Lijun, Liu Mingxing, *et al*.. Research progress of laser cladding amorphous coatings[J]. Laser and

Optoelectronics Progress, 2014, 51(7): 070002.
王彦芳, 肖丽君, 刘明星, 等. 激光熔覆制备非晶复合涂层的研究进展[J]. 激光与光电子学进展, 2014, 51(7): 070002.
3 Alam M M, Kaplan A F H, Tuominen J, *et al.*. Analysis of the stress raising action of flaws in laser clad deposits[J]. Materials & Design, 2013, 46: 328-337.
4 Wang Wei, Guo Pengfei, Zhang Jianzhong, *et al.*. Ultrasonic effect on laser cladding BT20 titanium alloy process[J]. Chinese J Lasers, 2013, 40(8): 0803004.
王 维, 郭鹏飞, 张建中, 等. 超声波对BT20钛合金激光熔覆过程的作用[J]. 中国激光, 2013, 40(8): 0803004.
5 Yang X J, Zhou J X, Ling X. Study on plastic damage of AISI 304 stainless steel induced by ultrasonic impact treatment[J]. Materials & Design, 2012, 36: 477-481.
6 Abdullah A, Malaki M, Eskandari A. Strength enhancement of the welded structures by ultrasonic peening[J]. Materials & Design, 2012, 38: 7-18.
7 Qiu C J, Zhang Y, Li Y, *et al.*. Influence of high-frequency micro-forging on surface residual stress of 304 stainless steel sample fabricated by laser prototyping[J]. Advanced Materials Research, 2012, 591: 1067-1070.
8 Lee H S, Kim D S, Jung J S, *et al.*. Influence of peening on the corrosion properties of AISI 304 stainless steel[J]. Corrosion Science, 2009, 51(12): 2826-2830.
9 Nie Xiangfan, He Weifeng, Zang Shunlai, *et al.*. Experimental study on improving high-cycle fatigue performance of TC11 titanium alloy by laser shock peening[J]. Chinese J Lasers, 2013, 40(8): 0803006.
聂祥攀, 何卫峰, 臧顺来, 等. 激光喷丸提高TC11钛合金高周疲劳性能的试验研究[J]. 中国激光, 2013, 40(8): 0803006.
10 Montemor M F. Functional and smart coatings for corrosion protection: A review of recent advances[J]. Surface and Coatings Technology, 2014, 258: 17-37.
11 Ralston K D, Fabijanic D, Birbilis N. Effect of grain size on corrosion of high purity aluminium[J]. Electrochimica Acta, 2011, 56(4): 1729-1736.

栏目编辑: 张浩佳